Journal Pre-proof

Finite element model validation based on an experimental model of the intact shoulder joint

Margarida Bola , José Simões , António Ramos

PII: S1350-4533(20)30168-5
DOI: https://doi.org/10.1016/j.medengphy.2020.11.004
Reference: JJBE 3582

To appear in: *Medical Engineering and Physics*

Received date: 12 January 2019
Revised date: 7 November 2020
Accepted date: 11 November 2020

Please cite this article as: Margarida Bola , José Simões , António Ramos , Finite element model validation based on an experimental model of the intact shoulder joint, *Medical Engineering and Physics* (2020), doi: https://doi.org/10.1016/j.medengphy.2020.11.004

Highlights

- A finite element model (FEM) of the intact shoulder was developed
- An experimental model of the intact shoulder was developed
- The FE model was successfully validated based on experimental results
- The experimental results suggest that load is transferred at the posterior region

Finite element model validation based on an experimental model of the intact shoulder joint

Margarida Bola[1], José Simões[1,2], António Ramos[1]

[1]TEMA, Biomechanics Research Group, Department of Mechanical Engineering, University of Aveiro, Portugal, Campo Universitário de Santiago, 3810-193 Aveiro

[2]ESAD- College of Art and Design, Avenida Calouste Gulbenkian, 4460-268 Senhora da Hora, Matosinhos, Portugal

* Corresponding author,

António Manuel Amaral Monteiro Ramos

Biomechanics research Group, University of Aveiro, 3810-193 Aveiro, Portugal,

E-mail: a.ramos@ua.pt

Abstract

The shoulder joint is a complex anatomical system. The main goal of this study was to build a Finite Element (FE) model of the intact shoulder joint and its validation was done using an experimental model comparing cortical strains. Considering the expected differences between the experimental model and an in vivo shoulder, the experimental model developed replicates adequately the in vivo functioning of the joint.

For the experimental model we used 4th generation composite bone structures of the humerus and scapula, including the humeral head cartilage, the glenoid cartilage and glenohumeral ligaments. The model also comprises the most important muscles in abduction. The FE model of the intact shoulder was developed mimicking the experimental model regarding the geometry of the bone structures.

Strain gauge rosettes were used to measure strain responses loading bone structures positioned in a 90° abduction angle. The accuracy of the strains calculated (numerical model) and measured (experimental model) was evaluated with linear regression analysis. The correlation coefficient of 0.76 and RMSE of 107 με indicate an adequate agreement between numerical and experimental strains.

The experimental procedure to simulate the biomechanics of the intact shoulder joint is a difficult task due to the instability of the joint and the number of structures that compose it. The use of FE models is necessary to perform more complex biomechanical studies, which are normally impossible to make with experimental ones, highlighting the importance of validation of FE models. The results of these models can then be used to compare with clinical data considering, however, the inherent characteristics of numerical simulations and differences relatively to clinical models.

Keywords: Intact shoulder, finite element model, experimental model, strain gage

Introduction

The development of accurate Finite Element (FE) models of the intact shoulder joint is a complex task due to the anatomy and biomechanics of the articulation. Some shoulder FE models available in literature [1,2] focus on the connection between the humerus and the scapula and several simplifications aim to reduce computational time, but with costs due to differences between the numerical model and the real scenario. Other FE models of the intact shoulder [3–6] consider realistic anatomical features, with joint stability achieved by means of muscles and by articular contact forces, allowing the humerus to move freely in the joint. However, there are FE models validated only against published results [4–6] and others that do not present any experimental validation [3].

Generally, experimental models of the shoulder consider a hanging humerus, which is activated in abduction by muscular loads applied to the deltoid and rotator cuff muscles [7,8]. Several strategies have been implemented for muscle force application, such as different force ratios [9], equal muscles forces [8–10], application of forces depending on the physiologic cross-sectional area of each muscle [10] or depending on electromyography results [8,10]. Commonly, muscle forces in experiments are applied by means of servo-hydraulic actuators [7,9,11,12] or by pneumatic muscles or weights [13–15].

The main goal of this study was to design an experimental model simulator of the intact shoulder to validate a FE model by comparing numerical with experimental strains.

Materials and Methods

Experimental shoulder model

The experimental shoulder model (see figure 1) was constructed with 4th generation composite bone structures, namely a left humerus and scapula, (Sawbones, Pacific Research Laboratories, Inc., Vashon Island, WA, USA). These composite structures replicate well the mechanical behavior of real bone and their material properties are within the same range [16].

The model includes the inferior glenohumeral ligament (IGHL), simulated by an elastic band (1.2 × 23.6 × 36 mm) that was glued to the bones (Figure 1). The elastic band was stretched 16.7 mm during humeral abduction (from 0º to 90°). The elastic modulus of the band was determined through a tensile test using a universal testing machine (Shimadzu). It was approximately 3.5 MPa, similar to 3 MPa presented in an in vivo study [17].

The cartilage of the experimental models was made in a three-step process: CAD model; CAD mold; and manufacturing. CAD models of both cartilages were made assuming a constant thickness of 0.95 mm in accordance with literature [18] and based on the observation of several CT scans. The CAD model was built considering the distance between the bone surfaces (glenoid cavity and humeral head). The synthetic cartilages (made of silicone rubber) were manufactured using room-temperature vulcanization silicone technique [19] and surfaces presented geometry accuracy [20].

The most important muscle forces in abduction were previously identified using a multi-body model of the intact shoulder (AnyBody software). The conditions simulating an adult male (weight: 101 kg, height: 1.61 m) performing an abduction motion (from 0° to 90°) with an external load of 10 N. Knowing the height (H) of the human body, the distance shoulder/hand was considered in accordance with the study of Roozbazar et al. (1979) [21]. Since the deltoid produces the greatest amount of force, it was divided into two lines of action (two cables) (figure 1). The rotator cuff muscles (supraspinatus, infraspinatus and subscapularis) were simulated with one line of action for each (three cables) but the insertion in the bones was made using a large band fixed in the same area, as previously adopted [2,8]. Muscle directions were anatomically defined, and two cable extremities were attached to the deltoid tuberosity with a large band glued to bone; three cable extremities were attached to the corresponding origin site of each rotator cuff muscle. The remaining cable extremities were attached to pneumatic muscles (DMSP-10-40N-AM-AM and DMSP-10-80N-AM-AM, FESTO) in force control.

The experimental model was based on previous studies [22,23] and performance was compared with literature [24]. The simulation of several degrees of abduction and stability of the joint are issues that deserve careful attention when performing the tests. The experiments performed with controlling muscular force allowed the necessary stability of the experimental setup and confirmed that the glenohumeral joint has high freedom.

Insert figure 1

<u>Experimental procedure</u>

The quasi-static testing apparatus (see Figure 2) was designed considering other experimental shoulder models [7,8,13]. The shoulder simulator was designed to replicate a humerothoracic angle of 90° of abduction, with the glenohumeral angle consistent with the scapular rhythm, since it is considered as a critical position for the glenohumeral joint [24]. Nevertheless, the rig allows the position of the joint in any abduction angle and to include the scapulothoracic rhythm. The humerus is equilibrated by the muscles and external forces that simulate the weight of arm and hand (see Figure 2). The muscle forces were monitored using a real-time controller (NI c-RIO-9074, National Instruments) and measured with a load cell (U9B, HBM) placed in line with the pneumatic muscles.

Insert figure 2

To analyze the strain responses of the shoulder model, strain gage rosettes (KFG-3-120-D17-11 L3M2S 3 mm, KFG-1-120-D17-11 L3M2S 1 mm, Kyowa Electronic Instruments Co.) were used. Two rosettes were glued on the scapula (anterior and posterior regions) and two on the humerus (close to the greater and lesser tubercles), as shown in Figure 3. The rosettes were connected to a data acquisition system PXI-1050 (National Instruments, Austin, TX, USA) controlled with a LabVIEW application. The maximum and minimum principal strains were calculated based on the measured signal of each rosette.

Insert figure 3

The shoulder testing device allows different strategies for force application, such as equal/different loads in all muscles, or absence of forces in some of them [2]. The external loads were applied on the extremity of the composite humeral bone at a distance of 277 mm (x_1) from the top of the humeral head. Since the mechanical system (bones and external load) is in equilibrium, an external force of 23.5 N was applied at point x_1 to balance the muscle forces. Due to pneumatic muscles constraints, it was not possible to apply 100 % of the previously determined muscle loads, so only 75 % of the load was applied, which corresponds to an external weight of 17.25 N. The average muscle forces used in the experiments are indicated in table 1.

Insert table 1

Bone structures were positioned on the experimental rig and the muscle forces were gradually added and applied to the muscle cables and the external weight was regularly added to the humeral shaft. The same experimental protocol was applied in all trials. The overall procedure was repeated seven times in each position.

Finite element model

The FE model was built based on the geometry of the cortical and cancellous structures of the composite bones (see Figure 2). The CAD model of cartilage was used to design and manufacture silicone molds to obtain the synthetic cartilage structures. The IGHL was numerically simulated to replicate the elastic band used in the experiments.

All components of the intact shoulder numerical model were considered having isotropic linear elastic behavior in the range of the loads applied [4,25]. Table 2 presents the material properties considered in the FE model.

Insert table 2

To reproduce the experimental shoulder model, the CAD representations were positioned in a way so that the scapula was fixed in the inferior angle and in the superior margin (figure 2), and a point of the humeral base was fixed to simulate the influence of the external load (reaction), as represented in Figure 4. The cortical /trabecular bone and cortical bone/cartilage interfaces were considered bonded in the FE model like the experimental models. The IGHL extremities were bonded to the cortical bone of the humerus and scapula.

A Coulomb contact friction $\mu = 0.2$ between the two cartilage (replicate) structures was considered due to the absence of synovial fluid. The consideration of such a high friction value used does not represent real (in vivo) conditions of healthy patients. The presence of synovial fluid and cartilage smoothness leads to lower friction and consequently lower contact pressures. However, the main aim of this study was to build a FE model that replicates the experimental model. For this reason, the contact friction coefficient considered mimics the friction between two synthetic silicone surfaces. Small-sliding formulation was considered, since little sliding between the silicone structures of the experimental model was observed. The same contact condition ($\mu = 0.2$) was used between the IGHL/cartilage interfaces. A pre-tension of 1.5 MPa was added to the IGHL model having in consideration the 3.5 MPa elastic modulus and 16.7 mm elongation.

Insert Figure 4

Muscle forces are the external loads applied to the FE model, similarly to what was done experimentally. The muscles considered were deltoid (two lines of action), infraspinatus, supraspinatus and subscapularis (one line of action each). The muscles lines of action are also represented in Figure 4. ABAQUS (Dassault Systèmes Simulia Corp, Providence, RI, USA) was the solver used.

A sensitivity analysis to obtain an adequate mesh convergence size was performed and is presented in figure 5. The FE model was built with linear tetrahedral elements of type C3D4 (4 nodes, 3 degrees of freedom per node). The selection of these finite elements were based on related published work [27,28]. The model had 427 845 degrees of freedom (142 615 nodes, 641 019 elements), presenting good accuracy with enough density [29]. To determine numerical strains, an average strain was considered from strains "picked" in 5 nodes of the equivalent region of the sensor of the experimental model. The percentage in terms of results and difference between them was calculated considering the experimental value as the base one.

Insert figure 5

Results

The humerus and scapula cortical strains measured experimentally are depicted in Figure 6. Regarding these results, a maximum principal strain of +139 $\mu\varepsilon$ and a minimum principal strain of -135 $\mu\varepsilon$ were measured in the anterior scapula (AS). For the posterior scapula (PS), a maximum principal strain of +353 $\mu\varepsilon$ and a minimum principal strain of -220 $\mu\varepsilon$ were measured. In the anterior humerus (AH), the experimental maximum and minimum principal strains were +86 $\mu\varepsilon$ and +17 $\mu\varepsilon$

respectively. As for the posterior humerus (PH), the maximum and minimum principal strain was +105 με and -74 με respectively.

Insert Figure 6

Concerning the scapula, the comparison between FE and experimental strains (see Figure 6) evidence that, in average, the FE model underestimates the maximum principal strains in -37% and overestimates the minimum principal strains in +67%. As for the humerus, the comparison shows that, in average, the FE model overestimates the maximum principal strains in +27% and underestimates the minimum principal strains in -560%.

It is important to evidence that the numerical minimum principal strain obtained with rosette AS (Anterior Scapula) is of compression nature (negative), while the equivalent experimental strain is of tension nature (positive, although of very low magnitude). This may indicate differences in the humerus positioning or a geometric variation in that region of the FE model, suggesting a more anterior position.

Discussion

As referred, the main objective with this study was to validate a FE model of the intact shoulder by comparing numerical-experimental strains. Even with some instability of the joint observed, the differences between numerical and experimental strains gives us the necessary confidence to use the FE model developed and tested for biomechanical studies as, for example, the differences of performance between different shoulder prostheses.

One way to validate different nature (numerical versus experimental) models is through the use of the correlation between experimental and numerical data expressed as the Root-Mean-Square-Error (RMSE). This indicator is usually used to measure the difference between values predicted by the FE model and the values measured with the experimental model. Considering all data points, we obtained a correlation coefficient of 0.77 and a RMSE of 107 με (see Figure 7). These results must be analyzed having in mind the complexity of the experimental model of the shoulder joint and number of components involved in the simulations. A detailed analysis on the strains obtained shows significant differences between the minimum principal strains at AS and AH, respectively +121% and -1113%. A possible explanation for these differences is the complexity of the geometry were sensors were placed, that possibly were not adequately replicated in the FE model as well as the inherent differences of stiffness between the numerical model and the experimental simulator. If these two points were excluded, differences higher than 100%, we would obtain a better correlation coefficient and a RMSE.

Insert Figure 7

Several authors have validated biomechanical models by comparing numerical and experimental maximum and minimum principal strains [1,30–33]. However, as far as we know, no model with both the humerus and the scapula has been experimentally validated. Nevertheless, we can, within certain limits, relate our study with those of Varghese *et al.* [32] and of Gupta *et al.* [1]. Gupta *et al.* [1] developed and validated a

3D FE model of a human scapula and obtained correlation coefficients between 0.89 and 0.97. Varghese *et al.* [32] validated FE models of long bones, including the humerus, and obtained correlation coefficients between 0.64 and 0.99. More adequate comparisons are difficult to perform because our experimental system takes into account two bone structures, different loading scenarios and boundary conditions when compared with other published studies.

The muscles simulated in our study allow us to analyze the shoulder in abduction. However, some loading scenarios are difficult to replicate in an experimental setup. The rig designed allows the simulation of the most critical position (90° abduction) of the shoulder with some degree of accuracy and repeatability. The experiments conducted confirmed that the glenohumeral joint is characterized by being highly free and of significant instability.

The experimental obtained evidence that, comparably, the scapula suffers much higher deformations than the humerus. The comparison of the results obtained with identical published is a non-straight forward exercise, mainly because, as far as we know, no studies consider the shoulder joint analyzed based on strain deformation, and instead focus on the biomechanical characterization of the joint before and after prosthesis implantation.

The biomechanical behavior of the scapula based on strains can be assessed on Maurel *et al.* [34,35] studies. Nonetheless, those studies consider only the behavior of the scapula when loaded in some exact locations (without considering the humerus) and no muscle actions were added to the experimental system. On the contrary, on the present study we analyze the behavior of the scapula and humerus strains due to their intrinsic relationship and under muscle loading. Therefore, the comparison of results with these studies is difficult or even not possible. In the present model, we observed that the posterior scapula presented higher deformations (in tension and in compression), in opposition to what Maurel *et al.* [34] observed in the intact scapula. In fact, during abduction, maximum principal strains were located mainly at the anterior and antero-superior regions of the scapula. This difference is probably related with the orientation of load and amount of force applied in these studies.

Our study presents some limitations, like the composite bone structures used that are adequate to replicate non-pathologic conditions, but are suitable to build experimental models. They present linear elastic behavior for the load conditions considered. These experimental models have homogeneous characteristics (geometry and materials) and are suitable to validate FE models for numerical simulations. A significant advantage of these bones is that they do not present geometric variability when comparing with cadaveric ones. Considerable differences on the proximal humerus shape [36] and glenoid cavity [37,38] is a reality in both non-pathologic and pathologic patients. This fact needs to be addressed when designing a surgery strategy to choose proper shoulder prosthesis.

Other limitation concern is the contact between components with silicon. In fact, this material presents high friction, which does not represent the real (in vivo) environment of healthy joints with synovial fluid and the cartilage smoothness leads to lower friction and consequently lower contact pressures. However, the aim of this study was to build a FE model that replicates the experimental one and this effect does not have any relevance concerning validation purpose. With a scientific confidence numerical model, any simulation can be made considering reliable physiological friction in the shoulder articulation.

Conclusions

The FE model developed validated using an experimental model, can be used to analyze the glenohumeral joint in several degrees of abduction to better understand the biomechanics of the shoulder articulation. Many factors can influence the usability of FE models, such as the ability of the CAD model to truly replicate all bone and muscle structures considered, their placement in the right position, origin and insertion site of the muscles and material properties. All these make the development of the intact FE model of the shoulder joint a difficult assignment to be accomplished. Nevertheless, this study proposes a FE model of the intact shoulder that was validated based on experimental data and can be applied to study the biomechanics of the intact and implanted shoulder for the analysis of prosthesis performance.

Acknowledgements

This work was supported by POCI-01-0145-FEDER-032486, funded by FEDER, through COMPETE2020 - (POCI), and by national funds (OE), through FCT/MCTES.

Conflict of Interest:

All authors disclose any financial and personal relationships with other people or organizations that could inappropriately influence the work. There are no known conflicts of interest.

Ethical Approval

Not required.

References

[1] Gupta S, van der Helm FCT, Sterk JC, van Keulen F, Kaptein BL. Development and experimental validation of a three-dimensional finite element model of the human scapula. Proc Inst Mech Eng H 2004;218:127–42. https://doi.org/10.1243/095441104322984022.

[2] Apreleva M, Parsons IM, Warner JJP, Fu FH, Woo SLY. Experimental investigation of reaction forces at the glenohumeral joint during active abduction. J Shoulder Elb Surg 2000;9:409–17. https://doi.org/10.1067/mse.2000.106321.

[3] Büchler P, Ramaniraka NA, Rakotomanana LR, Iannotti JP, Farron A. A finite element model of the shoulder: application to the comparison of normal and osteoarthritic joints. Clin Biomech 2002;17:630–9.

[4] Favre P, Senteler M, Hipp J, Scherrer S, Gerber C, Snedeker JG. An integrated model of active glenohumeral stability. J Biomech 2012;45:2248–55. https://doi.org/10.1016/j.jbiomech.2012.06.010.

[5] Terrier A, Reist A, Vogel A, Farron A. Effect of supraspinatus deficiency on humerus translation and glenohumeral contact force during abduction. Clin Biomech 2007;22:645–51. https://doi.org/10.1016/j.clinbiomech.2007.01.015.

[6] Walia P, Miniaci A, Jones MH, Fening SD. Theoretical Model of the Effect of Combined Glenohumeral Bone Defects on Anterior Shoulder Instability: A Finite Element Approach. J Orthop Res 2013:601–7. https://doi.org/10.1002/jor.22267.

[7] Bono CM, Renard R, Levine RG, Levy a S. Effect of displacement of fractures of the greater tuberosity on the mechanics of the shoulder. J Bone Joint Surg Br 2001;83:1056–62.

[8] Kedgley AE, Mackenzie GA, Ferreira LM, Drosdowech DS, King GJW, Faber KJ, et al. The effect of muscle loading on the kinematics of in vitro glenohumeral abduction. J Biomech 2007;40:2953–60. https://doi.org/10.1016/j.jbiomech.2007.02.008.

[9] Apreleva M, Parsons IM, Warner JJ, Fu FH, Woo SL. Experimental investigation of reaction forces at the glenohumeral joint during active abduction. J Shoulder Elbow Surg 2000;9:409–17. https://doi.org/10.1067/mse.2000.106321.

[10] Kedgley AE, Mackenzie G a, Ferreira LM, Drosdowech DS, King GJW, Faber KJ, et al. Humeral head translation decreases with muscle loading. J Shoulder Elbow Surg 2008;17:132–8. https://doi.org/10.1016/j.jse.2007.03.021.

[11] Kedgley AE, Mackenzie G a, Ferreira LM, Johnson J a, Faber KJ. In vitro kinematics of the shoulder following rotator cuff injury. Clin Biomech (Bristol, Avon) 2007;22:1068–73. https://doi.org/10.1016/j.clinbiomech.2007.06.005.

[12] Schamblin M, Gupta R, Yang BY, Mcgarry MH, Mcmaster WC, Lee TQ. Clinical Biomechanics In vitro quantitative assessment of total and bipolar shoulder arthroplasties : A biomechanical study using human cadaver shoulders. Clin Biomech 2009;24:626–31. https://doi.org/10.1016/j.clinbiomech.2009.05.007.

[13] Onder U, Blauth M, Kralinger F, Schmoelz W. Shoulder joint abduction motion test bench: A new shoulder test bench for in vitro experiments with active muscle force simulation. Biomed Tech 2012;57:163–8. https://doi.org/10.1515/bmt-2011-0119.

[14] Nyffeler RW, Sheikh R, Atkinson TS, Jacob HAC, Favre P, Gerber C. Effects of glenoid component version on humeral head displacement and joint reaction

forces : An experimental study. J Shoulder Elb Surg 2006;15:625–9. https://doi.org/10.1016/j.jse.2005.09.016.

[15] Jun BJ, Iannotti JP, McGarry MH, Yoo JC, Quigley RJ, Lee TQ. The effects of prosthetic humeral head shape on glenohumeral joint kinematics: a comparison of non-spherical and spherical prosthetic heads to the native humeral head. J Shoulder Elb Surg 2013;22:1423–32. https://doi.org/10.1016/j.jse.2013.01.002.

[16] Grover P, Albert C, Wang M, Harris GF. Mechanical characterization of fourth generation composite humerus. Proc Inst Mech Eng Part H J Eng Med 2011;225:1169–76. https://doi.org/10.1177/0954411911423346.

[17] Moore SM, Ellis B, Weiss J a., McMahon PJ, Debski RE. The Glenohumeral Capsule Should be Evaluated as a Sheet of Fibrous Tissue : A Validated Finite Element Model. Ann Biomed Eng 2010;38:66–76. https://doi.org/10.1007/s10439-009-9834-7.

[18] Fox JA, Cole BJ, Romeo AA, Meininger AK, Glenn RE, Bicos J, et al. Articular cartilage thickness of the humeral head: an anatomic study. Orthopedics 2008;31:216. https://doi.org/10.3928/01477447-20080301-11.

[19] Duarte RJ, Ramos A, Completo A, Relvas C, Simoes JA. The importance of femur/acetabulum cartilage in the biomechanics of the intact hip: experimental and numerical assessment. Comput Methods Biomech Biomed Engin 2013;18:880–9. https://doi.org/10.1080/10255842.2013.854335.

[20] Relvas C, Ramos A, Completo A, Simões JA. Accuracy control of complex surfaces in reverse engineering. Int J Precis Eng Manuf 2011;12:1035–42. https://doi.org/10.1007/s12541-011-0138-0.

[21] Roozbazar A, Bosker GW, Richerson ME. A theoretical model to estimate some ergonomic parameters from age, height and weight. Ergonomics 1979;22:43–58. https://doi.org/10.1080/00140137908924588.

[22] Sins L, Tétreault P, Hagemeister N, Nuño N. Adaptation of the AnyBody^{TM} Musculoskeletal Shoulder Model to the Nonconforming Total Shoulder Arthroplasty Context. J Biomech Eng 2015;137:101006. https://doi.org/10.1115/1.4031330.

[23] Lemieux PO, Nuño N, Hagemeister N, Tétreault P. Mechanical analysis of cuff tear arthropathy during multiplanar elevation with the AnyBody shoulder model. Clin Biomech 2012;27:801–6. https://doi.org/10.1016/j.clinbiomech.2012.04.008.

[24] Bergmann G, Graichen F, Bender A, Rohlmann A, Halder A, Beier A, et al. In vivo gleno-humeral joint loads during forward flexion and abduction. J Biomech 2011. https://doi.org/10.1016/j.jbiomech.2011.02.142.

[25] Maldonado ZM, Seebeck J, Heller MOW, Brandt D, Hepp P, Lill H, et al. Straining of the intact and fractured proximal humerus under physiological-like loading. J Biomech 2003;36:1865–73. https://doi.org/10.1016/S0021-9290(03)00212-4.

[26] Bola AM, Ramos A, Simões JA. Sensitivity analysis for finite element modeling of humeral bone and cartilage. Biomater Biomech Bioeng 2016;3:71–84.

[27] Comenda M, Quental C, Folgado J, Sarmento M, Monteiro J. Bone adaptation impact of stemless shoulder implants: a computational analysis. J Shoulder Elb Surg 2019;28:1886–96. https://doi.org/https://doi.org/10.1016/j.jse.2019.03.007.

[28] Virani NA, Harman M, Li K, Levy J, Pupello DR, Frankle MA. In vitro and finite element analysis of glenoid bone/baseplate interaction in the reverse shoulder design. J Shoulder Elb Surg 2008;17:509–21. https://doi.org/https://doi.org/10.1016/j.jse.2007.11.003.

[29] Ramos A, Simoes JA. Tetrahedral versus hexahedral finite elements in numerical modelling of the proximal femur. Med Eng Phys 2006;28:916–24. https://doi.org/10.1106/j.medengphy.2005.12.006.

[30] Helgason B, Taddei F, Pálsson H, Schileo E, Cristofolini L, Viceconti M, et al. A modified method for assigning material properties to FE models of bones. Med Eng Phys 2008;30:444–53. https://doi.org/10.1016/j.medengphy.2007.05.006.

[31] Taddei F, Schileo E, Helgason B, Cristofolini L, Viceconti M. The material mapping strategy influences the accuracy of CT-based finite element models of bones: an evaluation against experimental measurements. Med Eng Phys 2007;29:973–9. https://doi.org/10.1016/j.medengphy.2006.10.014.

[32] Varghese B, Short D, Penmetsa R, Goswami T, Hangartner T. Computed-tomography-based finite-element models of long bones can accurately capture strain response to bending and torsion. J Biomech 2011;44:1374–9. https://doi.org/10.1016/j.jbiomech.2010.12.028.

[33] Maurel N, Diop A, Grimberg J. A 3D finite element model of an implanted scapula : importance of a multiparametric validation using experimental data 2005;38:1865–72. https://doi.org/10.1016/j.jbiomech.2004.08.019.

[34] Maurel N, Diop A, Grimberg J, Elise S. In vitro biomechanical analysis of glenoids before and after implantation of prosthetic components. J Biomech 2002;35:1071–80. https://doi.org/10.1016/S0021-9290(02)00065-9.

[35] Diop A, Maurel N, Grimberg J, Gagey O. Influence of glenohumeral mismatch on bone strains and implant displacements in implanted glenoids. An in vitro experimental study on cadaveric scapulae. J Biomech 2006;39:3026–35. https://doi.org/10.1016/j.jbiomech.2005.10.015.

[36] Boileau P, Walch G. The three-dimensional geometry of the proximal humerus. Implications for surgical technique and prosthetic design. J Bone Joint Surg Br 1997;79:857–65. https://doi.org/<p>10.1302/0301-620X.79B5.7579</p>.

[37] Couteau B, Mansat P, Darmana R, Mansat M, Egan J. Morphological and mechanical analysis of the glenoid by 3D geometric reconstruction using computed tomography. Clin Biomech (Bristol, Avon) 2000;15 Suppl 1:S8-12.

[38] Mansat P, Bonnevialle N. Morphology of the normal and arthritic glenoid. Eur J Orthop Surg Traumatol 2013;23:287–99. https://doi.org/10.1007/s00590-012-1115-8.

List of figures

Figure 1

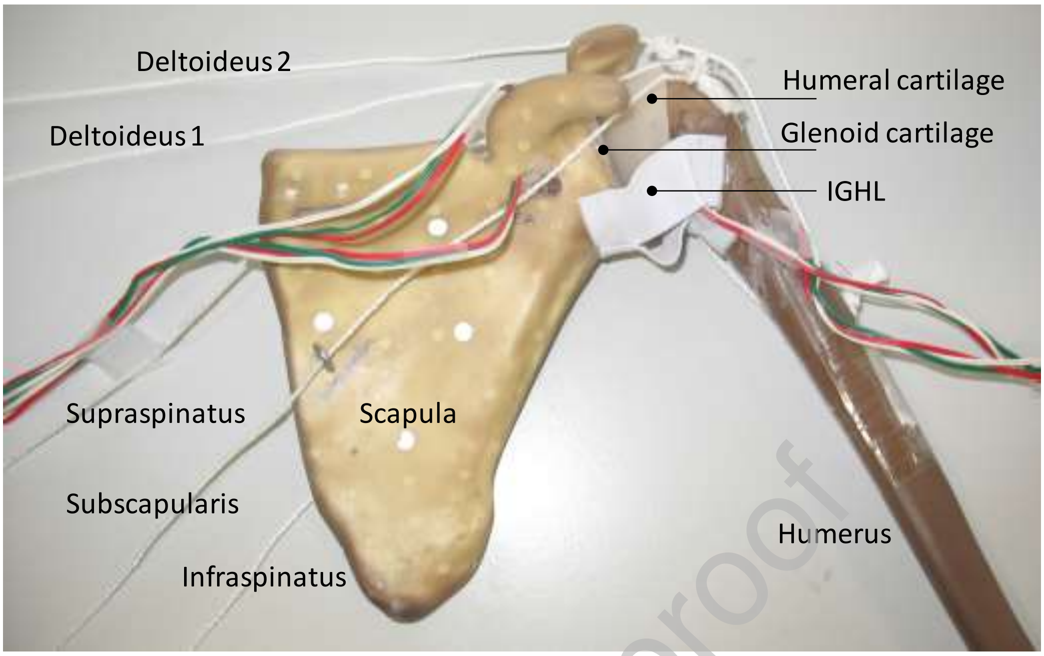
Deltoideus 2
Deltoideus 1
Humeral cartilage
Glenoid cartilage
IGHL
Supraspinatus
Scapula
Subscapularis
Infraspinatus
Humerus

Figure 2

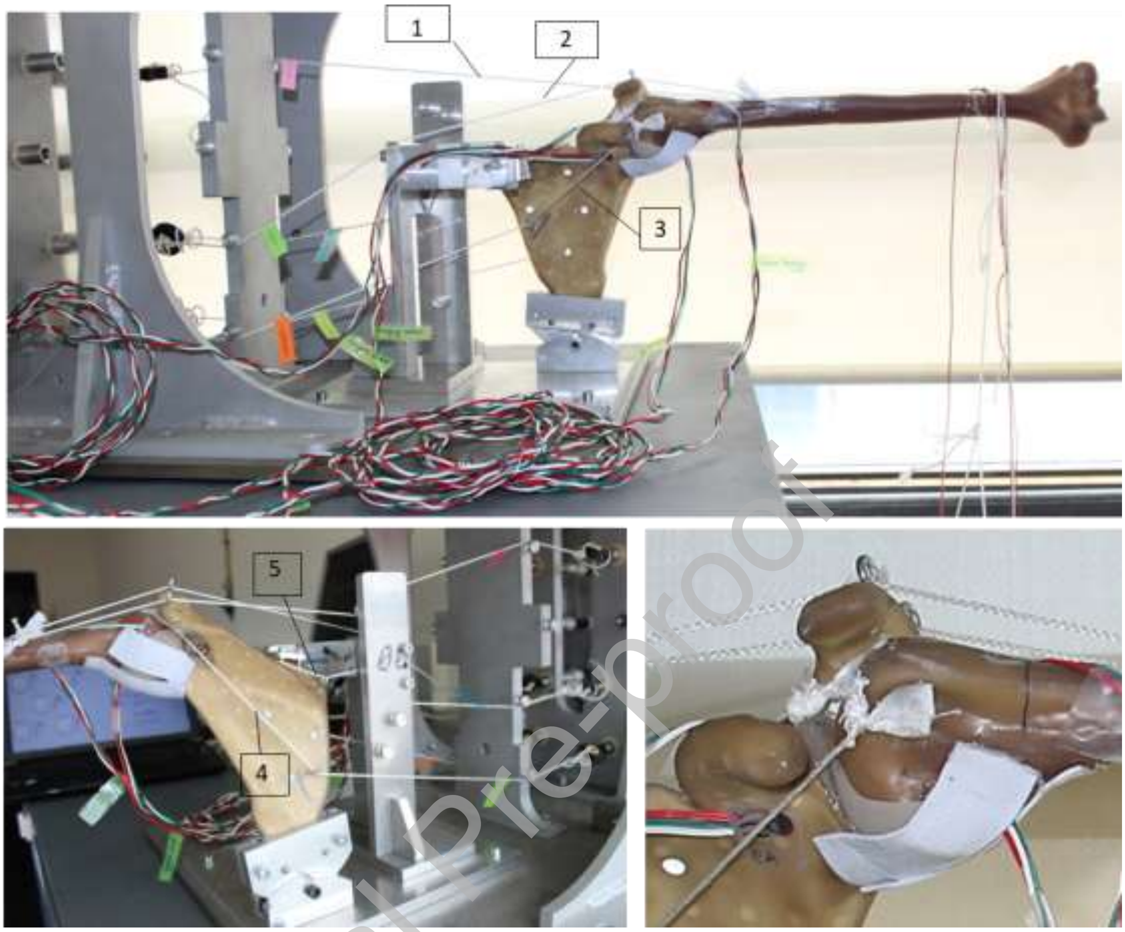

Figure 3

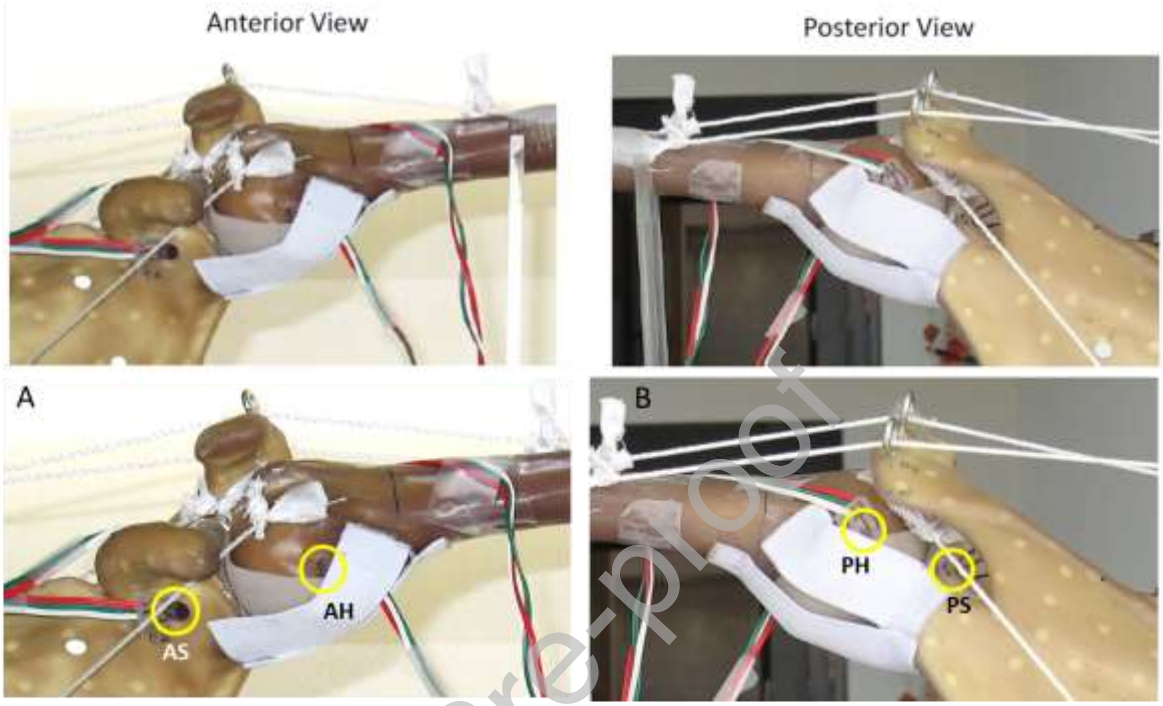

Figure 4

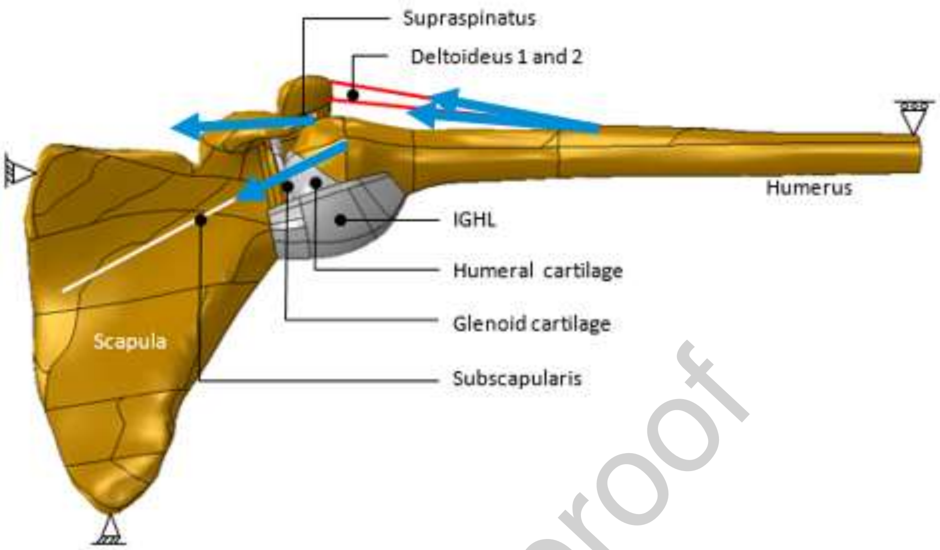
Supraspinatus
Deltoideus 1 and 2
Humerus
IGHL
Humeral cartilage
Glenoid cartilage
Subscapularis
Scapula

Figure 5

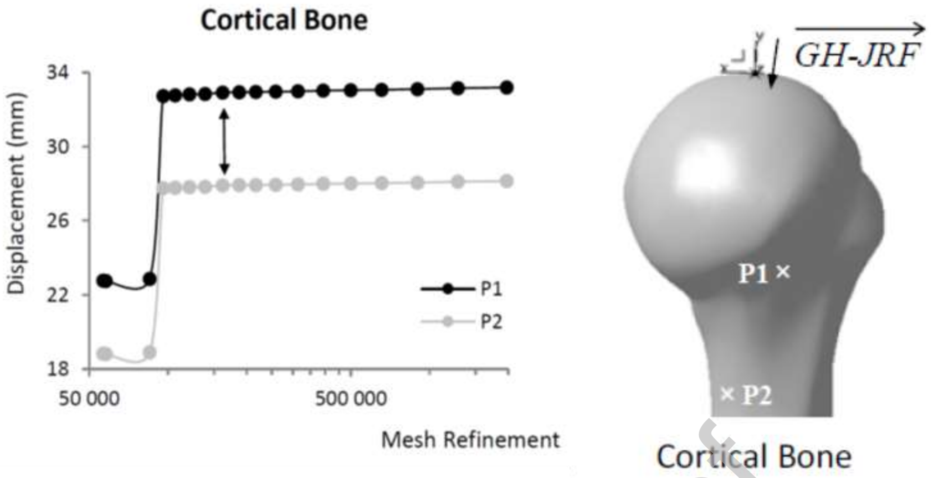
Cortical Bone
34
30
26
22
18
Displacement (mm)
50 000
500 000
Mesh Refinement
P1
P2
GH-JRF
P1 ×
× P2
Cortical Bone

Figure 6

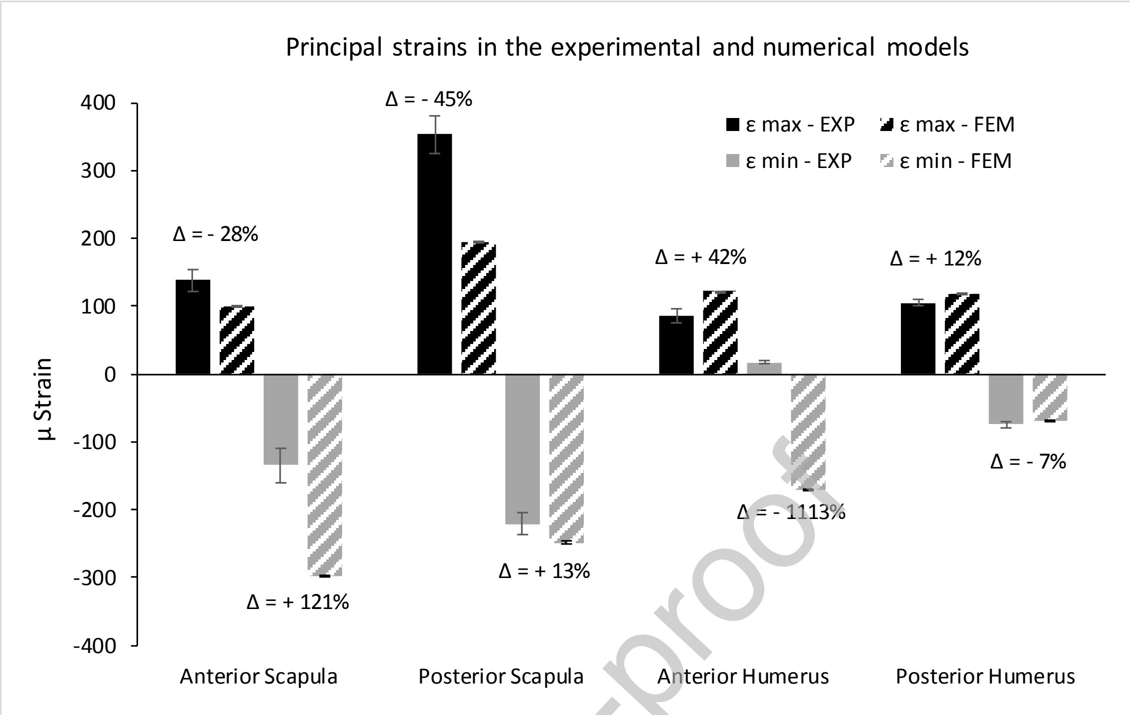
Principal strains in the experimental and numerical models
ε max - EXP
ε max - FEM
ε min - EXP
ε min - FEM
µ Strain
400
300
200
100
0
-100
-200
-300
-400
Δ = - 28%
Δ = + 121%
Δ = - 45%
Δ = + 13%
Δ = + 42%
Δ = - 1113%
Δ = + 12%
Δ = - 7%
Anterior Scapula
Posterior Scapula
Anterior Humerus
Posterior Humerus

Figure 7

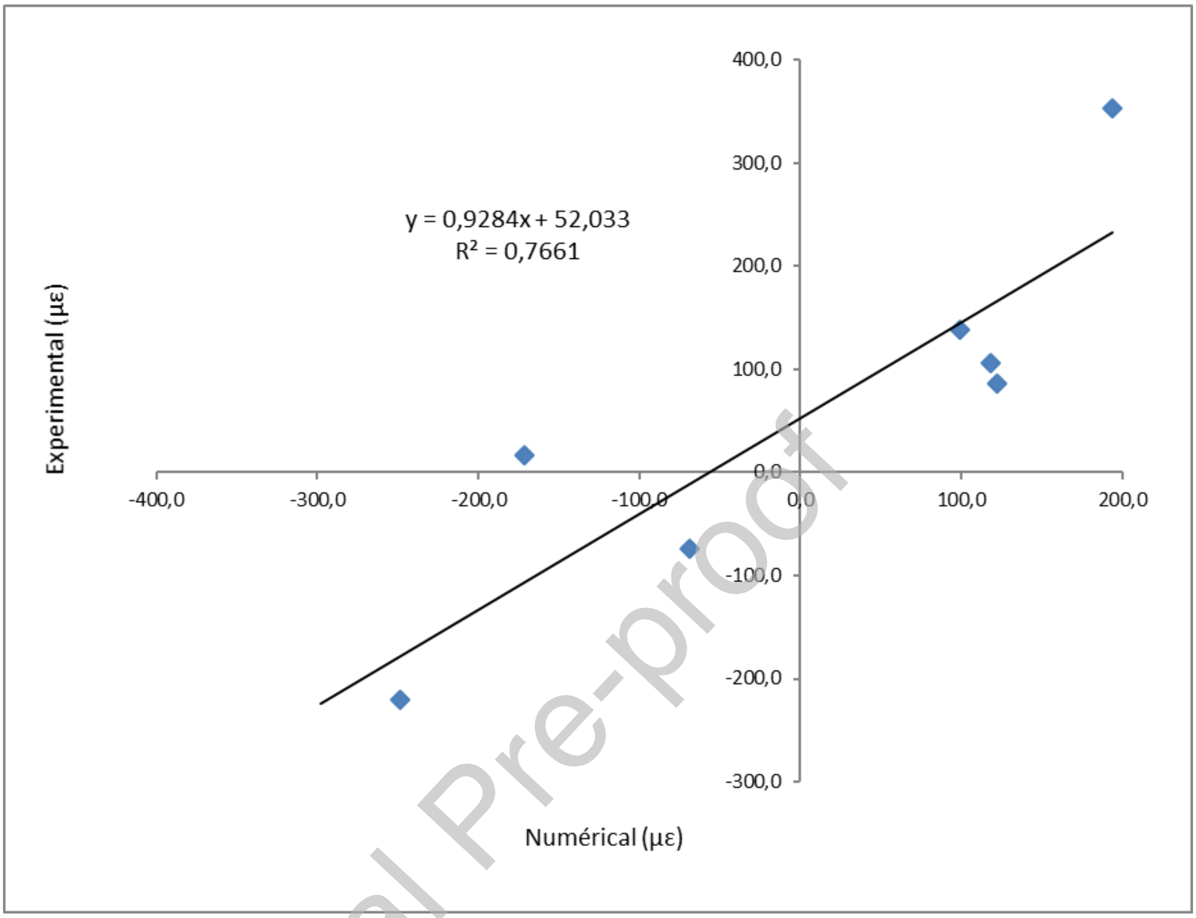
y = 0,9284x + 52,033
R² = 0,7661
Experimental (με)
Numérical (με)
400,0
300,0
200,0
100,0
0,0
-100,0
-200,0
-300,0
-400,0
-300,0
-200,0
-100,0
0,0
100,0
200,0

List of tables

Table 1 - Muscle forces used in the study.

Muscle	Theoretical Muscle Force [N] (75 %)	Average Muscle Force (SD) [N] Intact model
Deltoideus 1	113	110.92 (0.76)
Deltoideus 2	113	112.54 (1.39)
Subscapularis	169	168.14 (0.97)
Infraspinatus	90	88.90 (0.43)
Supraspinatus	68	67.08 (0.10)

Table 2

Table 2 - Material properties used in the FE model of the intact shoulder.

Structure	Young modulus	Poisson ratio
Composite cortical bone	16.7 GPa	0.3
Composite trabecular bone	0.155 GPa	0.3
Silicone (cartilage)	625 MPa	0.08
Elastic (IGHL)	3.5 MPa	0.09

Graphical Abstract

Experimental and Finite element model

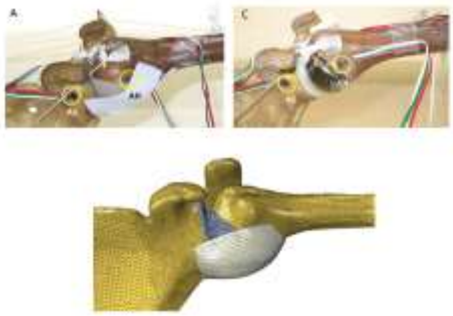

Comparison between Numeric VS Experimental